# Assessment of the exact-exchange-only Kohn-Sham method for the calculation of band structures for transition metal oxide and metal halide perovskites

Egor Trushin, Lukas Fromm, and Andreas Görling [*]

*Lehrstuhl für Theoretische Chemie, Universität Erlangen-Nürnberg, Egerlandstrasse 3, D-91058 Erlangen, Germany*

In the present paper we assess the performance of the exact-exchange-only (EXX) Kohn-Sham method to predict band structures of transition metal oxide and metal halide perovskites with the main emphasis on band gaps. For the considered set of prototypical systems with cubic structure, the performance of the EXX method for the prediction of band gaps is comparable with other popular methods for this purpose like density-functional calculations with the Heyd-Scuseria-Ernzerhof (HSE) hybrid functional and one-shot $GW$ ($G_0W_0$). Comparison with experimental values suggests that in the case of perovskites the EXX method, like HSE and $GW$ methods, should be supplemented by a treatment of electron-phonon effects. The EXX method is computationally more efficient than $G_0W_0$ and also provides post-self-consistent access to one-electron wave functions and band structures within the complete Brillouin zone with much lower computational effort than both $G_0W_0$ and hybrid DFT methods. We confirm the importance of including the higher-lying semicore shells within the explicitly treated states for halide perovskites which was already noted by earlier studies. Calculations taking into account only the valence space without the semicore states, however, remain still a reasonable option in practice. Spin-orbit coupling effects seem to be slightly underestimated in DFT calculations both with respect to $GW$ and experiment. The source of this underestimation can be of both technical and formal nature, and this point requires more critical consideration. For $CH_3NH_3PbI_3$, sizable Rashba spin splittings appear for the structure with the C-N bond of the methylammonium ion not lying along the long diagonal of the cubic unit cell.

## I. INTRODUCTION

The accurate prediction of electronic band structures of solids is a long-standing challenge for computational solid-state physics. Density-functional theory (DFT) within the Kohn-Sham (KS) formulation [1,2] relying on simple well-established exchange-correlation functionals based on the local-density approximation (LDA) or the generalized gradient approximation (GGA) has proven to be reliable for the description of the geometrical structure and accompanying energies for a wide range of materials at reasonable computational cost. However, DFT calculations with the LDA or GGA functionals provide electronic structures of typical semiconductors and insulators with substantially underestimated fundamental band gaps in comparison to experimental ones [3,4]. Due to this underestimation, electronic systems with small fundamental band gaps are frequently predicted to be metallic, i.e., to have a vanishing fundamental band gap. For the same reason, DFT calculations with the LDA or GGA functionals often cannot distinguish properly topological insulators and metals from trivial insulators [5].

Recent attempts to construct exchange-correlation functionals that better describe band structures of solids apply more sophisticated approximations using orbital-dependent density functionals [6–8]. These exchange-correlation functionals depend not only on the electron density and its derivatives with respect to spatial coordinates but also on the KS

orbitals or, going even further to more involved variants, on the KS wave function or KS state. Probably, the two most popular classes of orbital-dependent exchange-correlation functionals at present are meta-GGA [9–11] and hybrid functionals [12,13]. The additional ingredients in these functionals allow one to satisfy more exact constraints or fit reference data better, achieving higher accuracy. Some variants of orbital-dependent functionals indeed seem to give reasonable accuracies in calculations of band gaps [14–17]. Because the orbitals are functionals of the ground-state electron density, orbital-dependent functionals implicitly are density functionals, and the realm of DFT is not left. However, the construction of the local multiplicative KS exchange-correlation potential corresponding to orbital-dependent functionals is more involved than for LDA or GGA functionals and requires the optimized effective potential method. For meta-GGA and hybrid functionals this is typically not made, and instead, nonlocal exchange-correlation potentials are constructed as direct functional derivatives of the exchange-correlation energy with respect to the orbitals. Because the obtained exchange-correlation potentials are nonlocal, the resulting methods no longer are KS but generalized KS (GKS) methods [18] and as such still are proper DFT methods.

The main alternative to KS and GKS DFT for the first-principles calculation of the band structure of solids, which, however, is computationally demanding, starts from a KS reference band structure and uses the $GW$ method [19–21], i.e., applies many-body perturbation theory based on a set of Green's-function equations. The common procedure is to carry out the $GW$ calculations completely or partly

[*]andreas.goerling@fau.de

non-self-consistently, that is, to perform $G_0W_0$ or $GW_0$ calculations. In this case the obtained results depend significantly on the choice of the underlying KS method, i.e., the choice of the exchange-correlation functional in the calculation of the KS reference band structure [22]. Self-consistent $GW$ calculations, on the other hand, are not only computationally expensive but often yield worse results than $G_0W_0$ or $GW_0$ calculations for band gaps of solids [23,24]. Finally, the step to supplement self-consistent $GW$ calculations by vertex corrections [25] to increase the accuracy is computationally prohibitively expensive.

Hybrid DFT and $GW$ methods do not provide in a computationally economical way Bloch eigenstates and eigenvalues on a dense $k$-point grid in the Brillouin zone (BZ). Therefore, typically, extrapolation schemes have to be applied to a set of eigenstates and eigenvalues from a coarse $k$-point grid used in a regular calculation to evaluate spectral and Fermi surface properties, band structures along certain line in the BZ, etc. [26–28]. Although extrapolation schemes have shown their usefulness in many practical applications, the possibility to use data from a denser $k$-point grid can be beneficial in many situations to improve the quality of extrapolation or even to avoid it.

In the present work we apply the exact-exchange-only (EXX) KS method [8,29–33] that treats the KS exchange energy and potential exactly and neglects correlation. In contrast to meta-GGA and hybrid DFT methods the EXX method constructs the exact local multiplicative KS exchange potential by employing the optimized effective potential procedure [8,29–33] and does not use the Hartree-Fock-like nonlocal exchange potential, which would result from a straightforward derivative of the exchange energy with respect to the orbitals. The EXX method yields band structures of semiconductors that are much closer to experimental quasiparticle band structures than those of KS methods within the LDA or the GGA. Furthermore, EXX KS gaps of typical semiconductors reproduce experimental band gap with better quality than most of the popular hybrid functionals, except HSE06 (Heyd, Scuseria, Ernzerhof 2006), which provides a similar quality [31,34]. The self-consistent field (SCF) process to solve the EXX KS equations exhibits the same scaling of computational costs with the system size as the SCF process of hybrid functionals but with a lower prefactor if the diagonalization of the KS Hamiltonian matrix is carried out iteratively within each SCF step. The reason is that the KS exchange potential is a local, multiplicative potential, and its application on orbitals, once it is constructed, is as efficient as that of a LDA or GGA exchange potential and thus computationally much less demanding than acting with the nonlocal Hartree-Fock-like exchange potential on orbitals. This, moreover, is the reason why the post-SCF calculation of EXX band structures is as efficient as the calculation of LDA band structures. With the EXX method it is thus possible to highly efficiently evaluate post-SCF one-electron energies and orbitals on dense $k$-point grids within the BZ, which are required for many applications.

We also point out that the EXX method serves as the first step in a systematic path towards highly accurate exchange-correlation functionals, which in addition to an exact treatment of exchange use the adiabatic-connection fluctuation-dissipation (ACFD) theorem [35,36] to construct functionals

for the correlation energy. The simplest ACFD functional results from the direct random-phase approximation (dRPA) [37–40]. The dRPA is not self-interaction free and gives too negative total energies and poor atomization energies. Nonetheless, the EXX-dRPA approach, applied in a post-SCF manner using LDA or GGA orbitals and eigenvalues, was shown to provide good lattice constants, bulk moduli, and heats of formation for solids [41–43]. Because of the innate ability to treat van der Waals interaction, the EXX-dRPA approach has also shown good results in the description of surface and adsorption energies [43]. More recent applications of the EXX-dRPA approach include accurate predictions of fundamental band gaps [44] and the melting point of silicon [45]. By going beyond the dRPA the accuracy of ACFD methods can be significantly improved further [46–51]. However, these beyond-dRPA methods have so far been applied only to finite systems, i.e., atoms and molecules, or special cases like the homogeneous electron gas [50,51].

The band gap in the KS as well as in the GKS formalism is not equal to the quasiparticle band gap, the difference between ionization energy and electron affinity. The two band gaps differ by the derivative discontinuity of the exchange-correlation potential at integer electron numbers [52–55] which has to be added to the KS or GKS band gap in order to obtain the quasiparticle band gap. In approximate KS methods relying on the LDA or the GGA as well as in hybrid DFT methods, which are GKS methods, no derivative discontinuity is present for infinite periodic systems. That is, for these approximate DFT methods the KS or GKS band gap equals the quasiparticle band gap that would be obtained by total energy differences within the approximate method [3,4]. The lack of the derivative discontinuity is a formal shortcoming of LDA, GGA, and hybrid methods and means that a comparison of LDA, GGA, and hybrid band gaps with experimental quasiparticle band gaps makes the assumption that the errors due to the approximations in the exchange-correlation potential in these methods and the neglect of the derivative discontinuity cancel each other. This can be a better or worse assumption depending on the individual approximation. For the LDA and the GGA this assumption is apparently quite poor because their band gaps typically underestimate experimental band gaps considerably; for hybrid functionals the situation often looks better. In GKS approaches, indeed, one can argue that the unknown exact derivative discontinuity might be smaller [18].

EXX methods exhibit a derivative discontinuity. If exclusively the exchange contribution of the derivative discontinuity is added to EXX band gaps, much too large band gaps are obtained that are close to Hartree-Fock band gaps. The reason is that the correlation contribution to the discontinuity cancels the exchange contribution by a substantial amount. As mentioned above, it is possible to calculate the complete derivative discontinuity of the exchange-correlation potential at the EXX-dRPA level [44]. The resulting band gaps are very similar to $GW$ band gaps. However, the computational effort in this case also is similar. In this work we therefore consider EXX band gaps as estimates for the experimental band gaps. That is, we rely on a cancellation of the effects of the missing correlation potential and the derivative discontinuity. This is analogous to the practice in LDA, GGA, or hybrid methods and, as pointed out above, leads for the EXX method to band

gaps that are competitive in accuracy with those from the best hybrid methods, as documented by results for various semiconductors [34].

In this work, we consider electronic structures of a number of prototypical transition metal oxide and metal halide perovskites. These two families of perovskites are widely studied materials owing to their wide spectrum of interesting physical and chemical properties. Particularly, transition metal oxide perovskites are actively studied in the context of, e.g., metal-insulator transitions [56], superconductivity [57], and heterogeneous catalysis [58]. Meanwhile, metal halide perovskites have attracted extraordinary attention in recent years in the context of emerging photovoltaic technologies [59,60]. From a theoretical point of view, a proper description of their electronic properties is challenging and is still an area of active research. In comparison to typical semiconductors and insulators, additional factors appear which make a transparent comparison of calculated and experimental data difficult and, consequently, affect the judgment about the performance of individual methods. First, due to large computational costs, applications of *GW* and hybrid DFT methods to perovskites have been comparatively rare and are often affected by numerical convergence issues and approximations made in calculations. The necessity to take into account spin-orbit interactions (SOIs) further aggravates the situation. Furthermore, an important feature of transition metal oxide and metal halide perovskites is a sizable effect of lattice dynamics on electronic structure [61–64]. While first-principles calculations of electron-phonon interactions are gradually becoming more feasible and reliable [65,66], it is still unclear how accurately quantitative results of such calculations describe the effect of phonons on the electronic structure, in particular, because such calculations often cannot be fully converged nowadays.

## II. COMPUTATIONAL DETAILS

The EXX calculations were carried out with the Magnetization-Current Exact Exchange (MCEXX) program [67] based on norm-conserving pseudopotentials and plane-wave basis functions. The norm-conserving Troullier-Martins [68] EXX pseudopotentials employed in this work were generated with the code in Ref. [69]. The SOI is included in calculations of metal halide perovskites via the pseudopotentials [70]. The semicore $s$, $p$, and $d$ states of Ca, Sr, Ba, Zr, and Hf were treated as valence states. For Pb and Sn two configurations are considered with and without semicore $d$ electrons, whereas semicore $s$ and $p$ electrons were not included in valence space. All reported results were obtained using at least a $4 \times 4 \times 4$ $k$-point grid. When necessary, kinetic energy cutoffs up to 70 and 35 a.u. were used for the plane-wave basis sets for the KS orbitals and for the auxiliary basis sets to represent the exact KS exchange potentials and the KS response functions, respectively. From convergence tests we conclude that our band gaps are typically converged to 0.05 eV.

The Perdew-Burke-Ernzerhof (PBE) [71] and HSE06 [72] calculations presented in this paper were carried out using the Vienna Ab initio Simulation Package (VASP) [73–76] using the projector augmented wave method [77,78] for treating the core electrons. For Ca, Sr, Ba, Zr, Hf, Sn, Pb, and I, the $s$, $p$, and $d$ semicore states were treated as valence states. We have experienced convergence problem in calculations of $CsSnBr_3$ and $CsPbBr_3$ when the $s$ and $p$ semicore states of Br were treated as the valence states. Therefore, in Table II, PBE and HSE band gaps of these two systems are taken from pseudopotential calculations of Ref. [62], where the $s$ and $p$ semicore states were included in the valence space.

Except for hybrid organic-inorganic metal halide perovskites, the lattice parameters used in the calculations correspond to experimental values. Structures of hybrid organic-inorganic metal halide perovskites were taken from Ref. [79], where they were optimized by DFT calculations using the PBE exchange-correlation functional with the Tkatchenko-Scheffler correction [80] to take into account the long-range van der Waals interactions. For hybrid organic-inorganic perovskites, we use cubic structures obtained in Ref. [79]. The perovskites $CH_3NH_3PbI_3$ and $CH_3NH_3SnI_3$ both have two structures that are local energy minima with different orientations of the C-N bond of the methyl ammonium unit. In the first case (structure I), the C-N bond is oriented along the diagonal direction (111) of the cubic unit cell. In the second case (structure II), the C-N bond is located in the (020) plane and deviates from the face-to-face (100) direction by an angle which depends on chemical composition (see Ref. [79] for details).

## III. RESULTS AND DISCUSSION

### A. Transition metal oxide perovskites

We start by presenting results for transition metal oxide perovskites. In Table I, we summarize band gaps calculated with the PBE, HSE, and EXX functionals together with experimental values and $G_0W_0$ gaps from the literature. Calculated EXX band structures along the $\Gamma$–$X$–$M$–$\Gamma$–$R$–$X$ path in the BZ are shown in Fig. 1 together with those calculated with the PBE functional. As expected, band gaps calculated with PBE are substantially too small, whereas HSE, EXX, and $G_0W_0$ gaps are closer to experimental ones. HSE band gaps are, as a rule, smaller than those from EXX and $G_0W_0$. Systematically larger values of EXX KS gaps in comparison to the HSE ones were also found in Ref. [34] for various simple semiconductors. EXX and $G_0W_0$ yielded considerably overestimated band gaps on one part of the test set and underestimated those on the other part. While there is a sizable spread in reported $G_0W_0$ gaps, on average, $G_0W_0$ gaps seem to be the closest to experiment. A judgment on the relative performance of the considered methods, however, is not straightforward because significant corrections to band gap values, which are not considered in the present calculations, can be at least partially responsible for the deviations from experimental values. First, the magnitude of the renormalization of the band gaps due to zero-point motions of the nuclei, which is insignificant for typical semiconductors [93], seems to be substantial for transition metal oxide perovskites. For example, the zero-point motion correction for $SrTiO_3$ estimated in Ref. [94] leads to the band gap reduction of 0.3–0.4 eV. Similar phonon-induced renormalization of band gaps might be expected for some other considered materials due to the similar ionic nature of the bonding. Second, the SOI, which is not included in the

TABLE I. Calculated (PBE, HSE, and EXX) and experimental band gaps for transition metal oxide perovskites along with $G_0W_0$ band gaps from the literature.

| Compound | PBE | $G_0W_0$ | HSE | EXX | Expt. |
|---|---|---|---|---|---|
| $CaTiO_3$ | 2.35 | 3.62[a] | 3.47 | 4.23 | 3.57[b] |
| $SrTiO_3$ | 2.25 | 3.61[a], 4.08[c], 4.06[c], 3.55[c] | 3.48 | 4.18 | 3.4[d] |
| $BaTiO_3$ | 1.93 | 3.32[a], 3.8[e] | 3.33 | 3.91 | 3.2[f] |
| $SrZrO_3$ | 3.66 | 5.36[c], 5.29[c], 5.43[c] | 5.04 | 5.40 | 5.6[g] |
| $SrHfO_3$ | 4.04 | 5.69[c], 5.76[c], 5.81[c] | 5.42 | 6.03 | 6.1[h] |
| $BaZrO_3$ | 3.43 | 4.94[a] | 5.00 | 4.86 | 5.33[i] |
| $BaSnO_3$ | 1.42 | 3.05[e] | 2.71 | 3.38 | 2.9–3.0[j,k], 3.7[l] |

[a]Reference [81].
[b]Reference [82].
[c]Reference [83].
[d]Reference [84].
[e]Reference [85].
[f]Reference [86].
[g]Reference [87].
[h]Reference [88].
[i]Reference [89].
[j]Reference [90].
[k]Reference [91].
[l]Reference [92].

presented calculations of transition metal oxide perovskites due to the absence of corresponding $G_0W_0$ reference values, would reduce band gaps by about 0.2 eV for $SrHfO_3$ and up to 0.1 eV for other compounds. The finding that the EXX band gaps overestimate experimental band gaps therefore actually can be seen as a point indicating that the EXX band gaps are quite accurate. This is corroborated by the finding that in most cases (with the exception of $CaTiO_3$) $GW$ and EXX band gaps are not too far apart from each other.

We also note that the KS EXX gaps of 4.23, 4.18, and 3.91 eV for $CaTiO_3$, $SrTiO_3$, and $BaTiO_3$, respectively, calculated in the present work with pseudopotentials agree quite well with corresponding values of 4.28, 4.20, and 4.08 eV from the EXX all-electron full-potential linearized augmented plane wave calculations of Ref. [95]. This confirms the reliability of the pseudopotential approach in general and the scheme used in the present work to generate pseudopotentials in particular.

**B. Metal halide perovskites**

In Table II we summarize the band gaps of inorganic metal halide perovskites calculated with PBE, HSE, and EXX exchange-correlation functionals together with $G_0W_0$ band gaps from the literature. Results of calculations with and without the inclusion of SOI are shown. For these systems SOIs strongly affect the band structures and significantly diminish the band gap. The reduction of the band gap reaches up to about 0.5 and 1.5 eV for Sn- and Pb-containing systems, respectively.

The EXX band gap appears to be sensitive to the Sn $4d$ and Pb $5d$ states: the exclusion of semicore electrons changes the calculated band gap up to 0.1 and 0.25 eV for Sn- and Pb-containing systems, respectively. Changes of the same magnitude can appear in the EXX calculations of typical semiconductors when the size of the valence space is varied

[102]. A similar dependence of calculated band gaps of halide perovskites on the chosen valence electron configuration was already pointed out in the context of HSE and $G_0W_0$ calculations [62,103].

For inorganic metal halide perovskites the EXX band gaps are very close to those from $G_0W_0$ calculations. When semicore electrons are included in the calculations, the deviation between EXX KS gaps and $G_0W_0$ gaps in Ref. [62] obtained without SOIs does not exceed 0.05 eV for five of the six considered systems. The difference between EXX and $G_0W_0$ band gaps increases slightly upon inclusion of SOIs. As in the case of transition metal oxide perovskites, HSE again regularly produces smaller band gaps in comparison to EXX and $G_0W_0$. As expected, PBE yields band gaps that are even much smaller. For $CsSnI_3$ PBE even provides an incorrect band order when SOIs are included.

Figure 2 presents the EXX band structures obtained with and without SOI. Figure 2 shows that the changes in band structures due to SOI increase with the atomic numbers of the contained chemical elements. The reduction of band gaps upon the inclusion of SOI is very similar among PBE, HSE, and EXX, while for $G_0W_0$ a somewhat larger reduction is found. The fact that $GW$ yields larger SOI-induced reductions of the band gap in halide perovskites in comparison to local and semilocal DFT methods was mentioned previously in the literature (see, e.g., Refs. [62,103]). We are not aware of systematic investigations that consider how accurately DFT and $GW$ methods describe the effect of SOI in systems with heavy elements. It is known, however, that LDA tends to underestimate SOI effects for zinc-blende semiconductors containing heavy atoms [104]. That is why we assume that the effect of SOI in $GW$ calculations might be more reliable. However, the effect of SOI might be dependent not only on the applied computational method for the band structure but also on the schemes used to introduce SOI and to deal with core electrons. Moreover, a formally correct way to treat SOI in
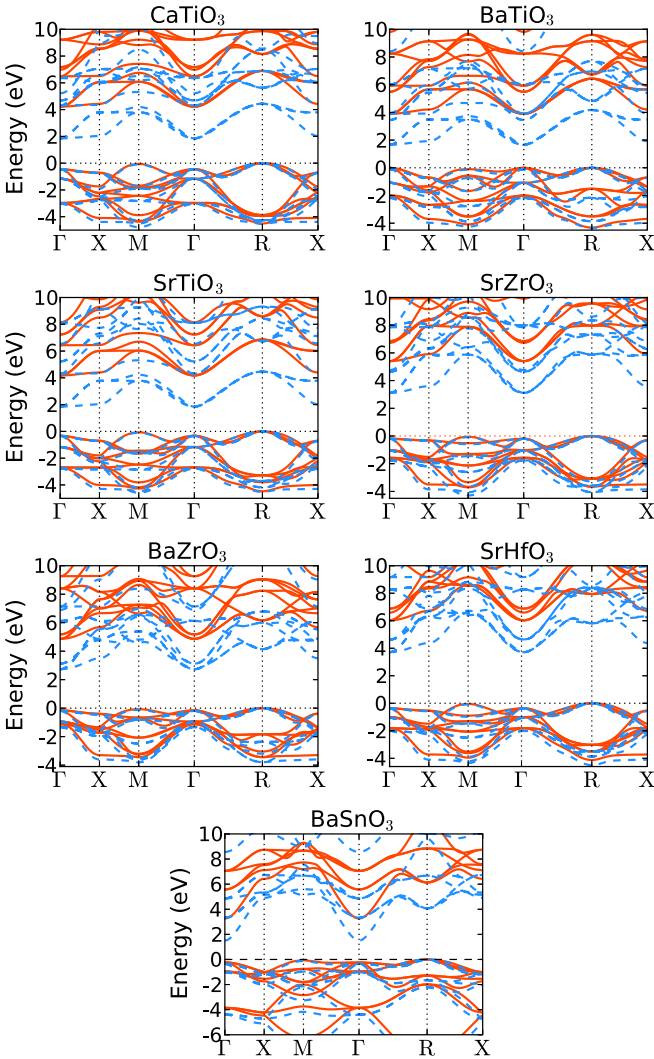
FIG. 1. Calculated band structures of transition metal oxide perovskites within PBE (dashed blue line) and EXX (solid red line).

Kohn-Sham formalism requires a generalization to spin-current DFT [70,105], and the inclusion of spin currents can lead to sizable changes, including the renormalization of the band gap up to at least several tenths of an eV [70].

A direct comparison of calculated zero-temperature band gaps with experimental values is, strictly speaking, inconsistent because cubic metal halide perovskites are stable only at room temperature or higher. All band gaps are calculated at the experimental lattice constant observed at finite temperature, which already includes thermal expansion, but the effects of vibrations and disorder are absent. In Ref. [62], the renormalization of band gaps due to vibrations and disorder was estimated and found to be quite large: up to about 0.6 eV. However, even if this renormalization is taken into account, the calculated HSE, EXX, and $G_0W_0$ gaps still substantially underestimate the experimental values. In order for metal halide perovskites to reach the predictive accuracy that EXX methods typically provide for simple semiconductors, the effect of the derivative discontinuity of both the exchange and the correlation potential probably has to be included. The EXX-dRPA approach of Ref. [44] might not be sufficient for this because it typically yields band gaps that are quite close to those from *GW* calculations, which similarly underestimate the band gaps of metal halide perovskites. A significant improvement toward experimental values in *GW*-based methods seems to be possible only when approximate vertex corrections are taken into account together with electron-phonon effects [62], which is computationally enormously expensive.

Band structures of hybrid organic-inorganic halide perovskites resemble closely those of the inorganic ones. An important difference, however, is the absence of spatial inversion symmetry leading to a lifting of the twofold spin degeneracy. Structure I, where the C-N bond is oriented along the long diagonal of the cubic unit cell, possesses small spin splittings akin to Dresselhaus spin splittings [107] of typical semiconductors. However, for structure II with the C-N bond located in the (020) plane, Rashba-like spin splittings [107] lead to a shift of the band extrema away from the *R* point of the BZ. The Rashba effect is more pronounced for $CH_3NH_3PbI_3$; Fig. 3 illustrates the situation. The present

TABLE II. Calculated (PBE, HSE, and EXX) and experimental band gaps for inorganic metal halide perovskites along with $G_0W_0$ band gaps from the literature, with (w SOI) and without (wo SOI) taking into account spin-orbit interaction.

| | PBE | | HSE | | $G_0W_0$ [96] | $G_0W_0$ [62] | | EXX wo semicore | | EXX w semicore | | |
|---|---|---|---|---|---|---|---|---|---|---|---|---|
| | wo SOI | w SOI | wo SOI | w SOI | wo SOI | wo SOI | w SOI | wo SOI | w SOI | wo SOI | w SOI | Expt. |
| $CsSnCl_3$ | 0.81 | 0.49 | 1.30 | 0.96 | 1.41 | 1.40 | 1.05 | 1.45 | 1.10 | 1.35 | 1.02 | 2.6[a] |
| $CsSnBr_3$ | 0.41[b] | 0.05[b] | 0.74[b] | | 0.81 | 1.02 | 0.68 | 1.02 | 0.71 | 0.98 | 0.67 | |
| $CsSnI_3$ | 0.36 | −0.02 | 0.64 | 0.23 | 0.56 | 0.82 | 0.31 | 0.85 | 0.41 | 0.84 | 0.37 | |
| $CsPbCl_3$ | 1.96 | 1.02 | 2.62 | 1.65 | 3.20 | 2.93 | 1.33 | 2.75 | 1.63 | 2.90 | 1.76 | 2.85[c] |
| $CsPbBr_3$ | 1.54[b] | 0.46[b] | 1.95[b] | | 2.50 | 2.56 | 0.94 | 2.27 | 0.98 | 2.43 | 1.09 | 2.36[d] |
| $CsPbI_3$ | 1.17 | 0.17 | 1.58 | 0.51 | 1.99 | 1.89 | 0.38 | 1.73 | 0.58 | 1.86 | 0.71 | 1.67[e], 1.73[f] |

[a]Reference [97].
[b]Reference [62].
[c]Reference [98].
[d]Reference [99].
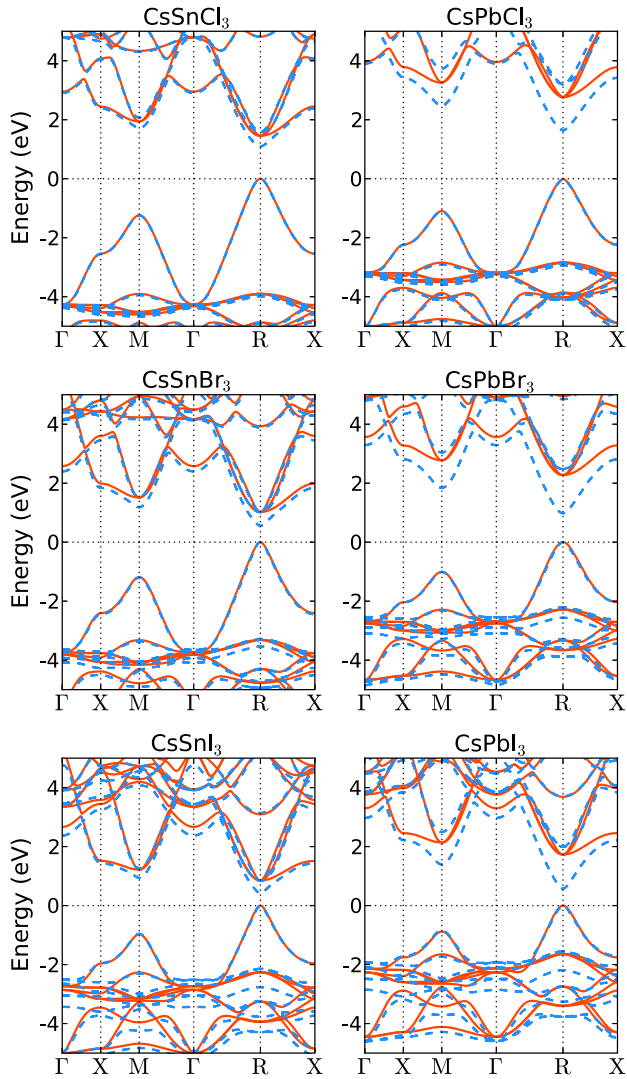[e]Reference [100].
[f]Reference [101].

FIG. 2. Calculated band structures of inorganic metal halide perovskites using EXX with (dashed blue line) and without (solid red line) spin-orbit coupling.

results on the dependence of spin splittings on the orientation of the methylammonium ion are in agreement with recently reported findings in Ref. [108] for $CH_3NH_3PbI_3$.

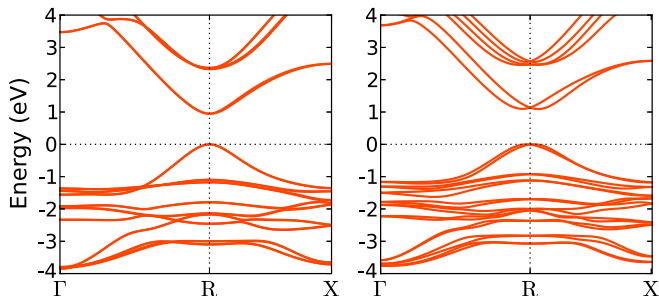Table III contains calculated band gaps for $CH_3NH_3PbI_3$ and $CH_3NH_3SnI_3$ for the two considered structures. As can



FIG. 3. Band structures of $CH_3NH_3PbI_3$ calculated within EXX including SOI for structure I (left) and structure II (right).

TABLE III. Calculated (PBE, HSE, and EXX) and experimental band gaps for hybrid organic-inorganic metal halide perovskites along with $G_0W_0$ band gaps from the literature, with and without taking into account spin-orbit interaction (SOI) and with (w semicore) or without (wo semicore) explicit treatment of Sn and Pb semicore $d$ electrons.

| | $CH_3NH_3SnI_3$ | | $CH_3NH_3PbI_3$ | |
|---|---|---|---|---|
| | Structure I | Structure II | Structure I | Structure II |
| PBE | 0.46 | 0.55 | 1.45 | 1.57 |
| PBE+SOI | 0.13 | 0.25 | 0.46 | 0.61 |
| HSE | 0.76 | 0.85 | 1.93 | 2.05 |
| HSE+SOI | 0.40 | 0.51 | 0.86 | 1.03 |
| EXX wo semicore | 0.93 | 1.00 | 2.05 | 2.16 |
| EXX+SOI wo semicore | 0.53 | 0.60 | 0.95 | 1.11 |
| EXX w semicore | 0.94 | 1.02 | 2.21 | 2.33 |
| EXX+SOI w semicore | 0.53 | 0.61 | 1.11 | 1.26 |
| $G_0W_0$+SOI | | | 1.16[a], 1.28[a] | |
| Expt. | | | 1.69[a] | |

[a]Reference [106].

be seen, the choice of crystal structure leads to differences of about 0.1 eV in the predicted band gap. The $G_0W_0$ gaps of $CH_3NH_3PbI_3$ are very close to those obtained within the EXX with the inclusion of Pb $5d$ electrons in valence space, whereas the experimental gap is about 0.4 eV larger.

## IV. CONCLUSIONS

The EXX KS method was applied to calculate band structures for a number of prototypical transition metal oxide and metal halide perovskites. It turned out that EXX KS calculations provide estimates for band gaps with quality comparable to other popular computational methods for this purpose, that is, DFT with the HSE hybrid functional and one-shot *GW* calculations. Indeed, EXX band gaps were found to be very close to $G_0W_0$ ones in most cases. From a formal point of view the presented results demonstrate that it is not necessary to leave the KS DFT framework and to turn to generalized KS approaches with hybrid functionals or to many-body perturbation theory with *GW* methods in order to obtain band structures with reasonable first estimates for band gaps. This has important practical implications. EXX calculations are computationally much more efficient than *GW* calculations and typically computationally somewhat less demanding than hybrid DFT calculations. In particular, the calculation of one-electron wave functions and their energy eigenvalues (bands) throughout the BZ subsequent to the SCF procedure is, within the EXX method, as efficient as in the case of LDA and GGA methods because the EXX exchange potential is a local multiplicative potential like the LDA or GGA one. As a result not only are routine calculations of band structures along high-symmetry lines of the BZ computationally highly economical, but so are many other potential post-SCF applications which require the one-electron wave functions and their energy eigenvalues on a dense $k$-point grid. The results of EXX calculations furthermore might be

interesting as a starting point for one-shot or partially self-consistent *GW* calculations when an LDA or PBE reference is inappropriate, as in the case of halide perovskites [109]. This option should be explored in future work.

Comparison with experimental data suggests that one has to take the electron-phonon effects into consideration to increase the predictive power of all considered computational approaches (HSE, EXX, *GW*) in band structure calculations of materials like perovskites that go beyond simple semiconductors. In the case of EXX, a supplemental treatment of correlation on the basis of the adiabatic-connection fluctuation-dissipation theorem preferred beyond the EXX-dRPA level [46–51,110] could be interesting. This is in line with *GW*-based calculations where reliable band gap estimation is achievable when both approximate vertex correction and electron-phonon effects are taken into account [62].

The present calculations confirm the importance of the choice of the valence electron space in calculations of halide perovskites which was already pointed out in the literature in the context of HSE and *GW* calculations [62,103]. More attention should be paid to the treatment of spin-orbit effects in halide perovskites as well as other systems with heavy elements. In this context, the approach to treat spin-orbit effects in conjunction with the treatment of core electrons is crucial [104]. For a formally consistent and numerically accurate description of spin-orbit interactions spin-current DFT should be used [70]. Spin-current DFT that takes into account spin-orbit-induced currents of the spin (magnetization) can lead to quantitative and even qualitative differences compared to standard DFT approaches taking into account only spin polarization or noncollinear spin [70]. The quality of current DFT- and *GW*-based computational approaches to treat spin-orbit interactions in solids containing heavy elements seems to be not sufficiently accessed at present.

For the hybrid organic-inorganic metal halide perovskites $CH_3NH_3PbI_3$ and $CH_3NH_3SnI_3$, we have found that the nature of spin splittings depends on the structure. Only ordinary Dresselhaus-like spin splittings appear for the structure with the C-N bond oriented along the long diagonal of the cubic unit cell, while the Rashba-like spin splittings, which are especially sizable in the case of $CH_3NH_3PbI_3$, emerge for the structure with the C-N bond located in the (020) plane and deviating from the face-to-face (100) direction.

[1] R. Parr and W. Yang, *Density-Functional Theory of Atoms and Molecules* (Oxford University Press, Oxford, 1994).

[2] R. M. Dreizler and E. K. U. Gross, *Density Functional Theory: An Approach to the Quantum Many-Body Problem* (Springer, Berlin, 1990).

[3] J. P. Perdew, Int. J. Quantum Chem. **28**, 497 (1985).

[4] J. P. Perdew, W. Yang, K. Burke, Z. Yang, E. K. U. Gross, M. Scheffler, G. E. Scuseria, T. M. Henderson, I. Y. Zhang, A. Ruzsinszky, H. Peng, J. Sun, E. Trushin, and A. Görling, Proc. Natl. Acad. Sci. USA **114**, 2801 (2017).

[5] J. Vidal, X. Zhang, L. Yu, J.-W. Luo, and A. Zunger, Phys. Rev. B **84**, 041109(R) (2011).

[6] E. Engel and R. M. Dreizler, *Density Functional Theory: An Advanced Course* (Springer, Berlin, 2011).

[7] S. Kümmel and L. Kronik, Rev. Mod. Phys. **80**, 3 (2008).

[8] A. Görling, J. Chem. Phys. **123**, 062203 (2005).

[9] J. Tao, J. P. Perdew, V. N. Staroverov, and G. E. Scuseria, Phys. Rev. Lett. **91**, 146401 (2003).

[10] J. P. Perdew, A. Ruzsinszky, G. I. Csonka, L. A. Constantin, and J. Sun, Phys. Rev. Lett. **103**, 026403 (2009).

[11] J. Sun, A. Ruzsinszky, and J. P. Perdew, Phys. Rev. Lett. **115**, 036402 (2015).

[12] J. P. Perdew, M. Ernzerhof, and K. Burke, J. Chem. Phys. **105**, 9982 (1996).

[13] J. Heyd, E. Scuseria, and M. Ernzerhof, J. Chem. Phys. **118**, 8207 (2003).

[14] F. Tran and P. Blaha, Phys. Rev. Lett. **102**, 226401 (2009).

[15] J. M. Crowley, J. Tahir-Kheli, and W. A. Goddard III, J. Phys. Chem. Lett. **7**, 1198 (2016).

[16] A. J. Garza and G. E. Scuseria, J. Phys. Chem. Lett. **7**, 4165 (2016).

[17] N. L. Nguyen, N. Colonna, A. Ferretti, and N. Marzari, Phys. Rev. X **8**, 021051 (2018).

[18] A. Seidl, A. Görling, P. Vogl, J. A. Majewski, and M. Levy, Phys. Rev. B **53**, 3764 (1996).

[19] M. S. Hybertsen and S. G. Louie, Phys. Rev. B **34**, 5390 (1986).

[20] G. Onida, L. Reining, and A. Rubio, Rev. Mod. Phys. **74**, 601 (2002).

[21] F. Bechstedt, F. Fuchs, and G. Kresse, Phys. Status Solidi B **246**, 1877 (2009).

[22] F. Fuchs, J. Furthmüller, F. Bechstedt, M. Shishkin, and G. Kresse, Phys. Rev. B **76**, 115109 (2007).

[23] A. L. Kutepov, Phys. Rev. B **95**, 195120 (2017).

[24] M. Grumet, P. Liu, M. Kaltak, J. Klimeš, and G. Kresse, Phys. Rev. B **98**, 155143 (2018).

[25] M. Shishkin, M. Marsman, and G. Kresse, Phys. Rev. Lett. **99**, 246403 (2007).

[26] J. R. Yates, X. Wang, D. Vanderbilt, and I. Souza, Phys. Rev. B **75**, 195121 (2007).

[27] D. R. Hamann and D. Vanderbilt, Phys. Rev. B **79**, 045109 (2009).

[28] G. K. Madsen, J. Carrete, and M. J. Verstraete, Comput. Phys. Commun. **231**, 140 (2018).

[29] R. T. Sharp and G. K. Horton, Phys. Rev. **90**, 317 (1953).

[30] J. D. Talman and W. F. Shadwick, Phys. Rev. A **14**, 36 (1976).

[31] M. Städele, J. A. Majewski, P. Vogl, and A. Görling, Phys. Rev. Lett. **79**, 2089 (1997).

[32] A. Görling, Phys. Rev. Lett. **83**, 5459 (1999).

[33] M. Städele, M. Moukara, J. A. Majewski, P. Vogl, and A. Görling, Phys. Rev. B **59**, 10031 (1999).

[34] E. Trushin and A. Görling, Eur. Phys. J. B **91**, 149 (2018).

[35] D. C. Langreth and J. P. Perdew, Solid State Commun. **17**, 1425 (1975).

[36] D. C. Langreth and J. P. Perdew, Phys. Rev. B **15**, 2884 (1977).

[37] F. Furche, Phys. Rev. B **64**, 195120 (2001).

[38] M. Fuchs and X. Gonze, Phys. Rev. B **65**, 235109 (2002).

[39] A. Heßelmann and A. Görling, Mol. Phys. **108**, 359 (2010).

[40] X. Ren, P. Rinke, C. Joas, and M. Scheffler, J. Mater. Sci. **47**, 7447 (2012).

[41] J. Harl and G. Kresse, Phys. Rev. Lett. **103**, 056401 (2009).

[42] J. Harl, L. Schimka, and G. Kresse, Phys. Rev. B **81**, 115126 (2010).

[43] L. Schimka, J. Harl, A. Stroppa, A. Grüneis, M. Marsman, F. Mittendorfer, and G. Kresse, Nat. Mater. **9**, 741 (2010).

[44] E. Trushin, M. Betzinger, S. Blügel, and A. Görling, Phys. Rev. B **94**, 075123 (2016).

[45] F. Dorner, Z. Sukurma, C. Dellago, and G. Kresse, Phys. Rev. Lett. **121**, 195701 (2018).

[46] A. Grüneis, M. Marsman, J. Harl, L. Schimka, and G. Kresse, J. Chem. Phys. **131**, 154115 (2009).

[47] X. Ren, A. Tkatchenko, P. Rinke, and M. Scheffler, Phys. Rev. Lett. **106**, 153003 (2011).

[48] P. Bleiziffer, M. Krug, and A. Görling, J. Chem. Phys. **142**, 244108 (2015).

[49] J. Erhard, P. Bleiziffer, and A. Görling, Phys. Rev. Lett. **117**, 143002 (2016).

[50] M. Hellgren and U. von Barth, J. Chem. Phys. **132**, 044101 (2010).

[51] N. Colonna, M. Hellgren, and S. de Gironcoli, Phys. Rev. B **90**, 125150 (2014).

[52] J. P. Perdew, R. G. Parr, M. Levy, and J. L. Balduz, Phys. Rev. Lett. **49**, 1691 (1982).

[53] J. P. Perdew and M. Levy, Phys. Rev. Lett. **51**, 1884 (1983).

[54] L. J. Sham and M. Schlüter, Phys. Rev. Lett. **51**, 1888 (1983).

[55] A. Görling, Phys. Rev. B **91**, 245120 (2015).

[56] M. Imada, A. Fujimori, and Y. Tokura, Rev. Mod. Phys. **70**, 1039 (1998).

[57] Y. Tokura, Phys. Today **56**(7), 50 (2003).

[58] J. Zhu, H. Li, L. Zhong, P. Xiao, X. Xu, X. Yang, Z. Zhao, and J. Li, ACS Catal. **4**, 2917 (2014).

[59] M. A. Green, A. Ho-Baillie, and H. J. Snaith, Nat. Photonics **8**, 506 (2014).

[60] M. Grätzel, Nat. Mater. **13**, 838 (2014).

[61] W. A. Saidi, S. Ponce, and B. Monserrat, J. Phys. Chem. Lett. **7**, 5247 (2016).

[62] J. Wiktor, U. Rothlisberger, and A. Pasquarello, J. Phys. Chem. Lett. **8**, 5507 (2017).

[63] S. McKechnie, J. M. Frost, D. Pashov, P. Azarhoosh, A. Walsh, and M. van Schilfgaarde, Phys. Rev. B **98**, 085108 (2018).

[64] W. A. Saidi and A. Kachmar, J. Phys. Chem. Lett. **9**, 7090 (2018).

[65] F. Giustino, Rev. Mod. Phys. **89**, 015003 (2017).

[66] B. Monserrat, J. Phys.: Condens. Matter **30**, 083001 (2018).

[67] The MCEXX (Magnetization Current Exact-Exchange) code is a pseudopotential plane-wave code developed at the University of Erlangen-Nuremberg.

[68] N. Troullier and J. L. Martins, Phys. Rev. B **43**, 1993 (1991).

[69] E. Engel, A. Höck, R. N. Schmid, R. M. Dreizler, and N. Chetty, Phys. Rev. B **64**, 125111 (2001).

[70] E. Trushin and A. Görling, Phys. Rev. B **98**, 205137 (2018).

[71] J. P. Perdew, K. Burke, and M. Ernzerhof, Phys. Rev. Lett. **77**, 3865 (1996).

[72] A. V. Krukau, O. A. Vydrov, A. F. Izmaylov, and G. E. Scuseria, J. Chem. Phys. **125**, 224106 (2006).

[73] G. Kresse and J. Hafner, Phys. Rev. B **47**, 558 (1993).

[74] G. Kresse and J. Hafner, Phys. Rev. B **49**, 14251 (1994).

[75] G. Kresse and J. Furthmüller, Comput. Mater. Sci. **6**, 15 (1996).

[76] G. Kresse and J. Furthmüller, Phys. Rev. B **54**, 11169 (1996).

[77] P. E. Blöchl, Phys. Rev. B **50**, 17953 (1994).

[78] G. Kresse and D. Joubert, Phys. Rev. B **59**, 1758 (1999).

[79] J. Li and P. Rinke, Phys. Rev. B **94**, 045201 (2016).

[80] A. Tkatchenko and M. Scheffler, Phys. Rev. Lett. **102**, 073005 (2009).

[81] A. Gierlich, Ph.D. thesis, RWTH Aachen University, 2011.

[82] K. Ueda, H. Yanagi, R. Noshiro, H. Hosono, and H. Kawazoe, J. Phys.: Condens. Matter **10**, 3669 (1998).

[83] Z. Ergönenc, B. Kim, P. Liu, G. Kresse, and C. Franchini, Phys. Rev. Mater. **2**, 024601 (2018).

[84] S. Zollner, A. A. Demkov, R. Liu, P. L. Fejes, R. B. Gregory, P. Alluri, J. A. Curless, Z. Yu, J. Ramdani, R. Droopad, T. E. Tiwald, J. N. Hilfiker, and J. A. Woollam, J. Vac. Sci. Technol. **18**, 2242 (2000).

[85] H. Li, I. E. Castelli, K. S. Thygesen, and K. W. Jacobsen, Phys. Rev. B **91**, 045204 (2015).

[86] S. H. Wemple, Phys. Rev. B **2**, 2679 (1970).

[87] Y. S. Lee, J. S. Lee, T. W. Noh, D. Y. Byun, K. S. Yoo, K. Yamaura, and E. Takayama-Muromachi, Phys. Rev. B **67**, 113101 (2003).

[88] M. Sousa, C. Rossel, C. Marchiori, H. Siegwart, D. Caimi, J.-P. Locquet, D. J. Webb, R. Germann, J. Fompeyrine, K. Babich, J. W. Seo, and C. Dieker, J. Appl. Phys. **102**, 104103 (2007).

[89] J. Robertson, J. Vac. Sci. Technol. **18**, 1785 (2000).

[90] H. J. Kim, U. Kim, T. H. Kim, J. Kim, H. M. Kim, B.-G. Jeon, W.-J. Lee, H. S. Mun, K. T. Hong, J. Yu, K. Char, and K. H. Kim, Phys. Rev. B **86**, 165205 (2012).

[91] S. A. Chambers, T. C. Kaspar, A. Prakash, G. Haugstad, and B. Jalan, Appl. Phys. Lett. **108**, 152104 (2016).

[92] B. S. Joo, Y. J. Chang, L. Moreschini, A. Bostwick, E. Rotenberg, and M. Han, Curr. Appl. Phys. **17**, 595 (2017).

[93] F. Karsai, M. Engel, G. Kresse, and E. Flage-Larsen, New J. Phys. **20**, 123008 (2018).

[94] C. Bhandari, M. van Schilgaarde, T. Kotani, and W. R. L. Lambrecht, Phys. Rev. Mater. **2**, 013807 (2018).

[95] M. Betzinger, C. Friedrich, A. Görling, and S. Blügel, Phys. Rev. B **85**, 245124 (2012).

[96] Y. Ying, X. Luo, and H. Huang, J. Phys. Chem. C **122**, 17718 (2018).

[97] L. Peedikakkandy and P. Bhargava, RSC Adv. **6**, 19857 (2016).

[98] M. Sebastian, J. A. Peters, C. C. Stoumpos, J. Im, S. S. Kostina, Z. Liu, M. G. Kanatzidis, A. J. Freeman, and B. W. Wessels, Phys. Rev. B **92**, 235210 (2015).

[99] J. B. Hoffman, A. L. Schleper, and P. V. Kamat, J. Am. Chem. Soc. **138**, 8603 (2016).

[100] C. C. Stoumpos, C. D. Malliakas, and M. G. Kanatzidis, Inorg. Chem. **52**, 9019 (2013).

[101] G. E. Eperon, S. D. Stranks, C. Menelaou, M. B. Johnston, L. M. Herz, and H. J. Snaith, Energy Environ. Sci. **7**, 982 (2014).

[102] E. Engel, Int. J. Quantum Chem. **116**, 867 (2016).

[103] M. R. Filip and F. Giustino, Phys. Rev. B **90**, 245145 (2014).

[104] P. Carrier and S.-H. Wei, Phys. Rev. B **70**, 035212 (2004).

[105] K. Bencheikh, J. Phys. A **36**, 11929 (2003).

[106] C. Quarti, E. Mosconi, J. M. Ball, V. D'Innocenzo, C. Tao, S. Pathak, H. J. Snaith, A. Petrozza, and F. De Angelis, Energy Environ. Sci. **9**, 155 (2016).

[107] R. Winkler, *Spin-Orbit Coupling Effects in Two-Dimensional Electron and Hole Systems* (Springer, Berlin, 2003).

[108] K. Frohna, T. Deshpande, J. Harter, W. Peng, B. A. Barker, J. B. Neaton, S. G. Louie, O. M. Bakr, D. Hsieh, and M. Bernardi, Nat. Commun. **9**, 1829 (2018).

[109] L. Leppert, T. Rangel, and J. B. Neaton, arXiv:1903.11376.

[110] A. Görling, Phys. Rev. B **99**, 235120 (2019).